Phosphorescent Cyclometalated Iridium(III) Complexes Bearing Ethynyl-Extended 2-(2'-Hydroxyphenyl) Benzoxazole Ancillary Ligands

Julien Massue, Gilles Ulrich, Filippo Monti, Andrea Barbieri

Phosphorescent Cyclometalated Iridium(III) Complexes Bearing Ethynyl-Extended 2-(2'-Hydroxyphenyl) Benzoxazole Ancillary Ligands

Julien Massue,*[a] Gilles Ulrich,[a] Filippo Monti,[b] and Andrea Barbieri*[b]

[a] Dr. J. Massue, Dr. G. Ulrich
Institut de Chimie et Procédés pour l'Energie, l'Environnement et la Santé (ICPEES), UMR CNRS 7515
Ecole Européenne de Chimie, Polymères et Matériaux (ECPM)
25 Rue Becquerel, 67087 Strasbourg Cedex 02, France
E-mail: massue@unistra.fr

[b] Dr. F. Monti, Dr. A. Barbieri
Istituto per la Sintesi Organica e la Fotoreattività (ISOF)
Consiglio Nazionale delle Ricerche (CNR)
Via Gobetti 101, 40129 Bologna, Italy
E-mail: andrea.barbieri@isof.cnr.it

Supporting information for this article is given via a link at the end of the document.

Abstract: This article describes the synthesis and full photophysical studies at room and low temperature of a series of iridium(III) complexes incorporating an ethynyl-extended benzoxazole-based ancillary ligand. The electronic nature of the terminal end-group of the ligand around the metallic ion was modulated by the simple introduction of electron-donating (Me, NBu_2) or -withdrawing (CN) groups. For all complexes, TD-DFT calculations showed that the lowest-lying transition was ligand-centered and that the nature of the first triplet state was very sensitive to electronic parameters leading to a charge transfer (CT) or locally excited (LE) excited-state, always centered on the ancillary ligand. Singlet oxygen sensitization studies were performed on all compounds, showing that iridium(III) complexes containing cyano-functionalized ligands feature sensitization parameters, making them attractive candidates for photodynamic therapy.

Introduction

Cyclometalated iridium(III) complexes displaying sizable phosphorescence emission have been the focus of intense research due to their strategic position at the crossroad of many attractive applications. These phosphorescent emitters have been indeed beneficially used in applicative fields including optoelectronics,[1-5] non-linear optics,[6] sensing,[7-10] or as particularly biocompatible probes for in vitro bioimaging.[11-13] This interest is largely due to the possibility to fine-tune their photophysical properties depending on subtle electronic modifications on the π-conjugated backbone of the ligands coordinated to the metal.[14-17] Indeed, cyclometalated complexes have been shown to feature a strong interplay between the molecular orbitals of the ancillary ligands and those of the metallic center, leading to either Metal-to-Ligand Charge Transfer (MLCT) or Ligand-to-Ligand Charge Transfer (LLCT) intense transitions. Electronic modifications around the trivalent iridium ion can indeed lead to drastic optical parameter changes such as absorption and/or emission maximum wavelength, phosphorescent quantum yields or excited-state lifetimes. Decorated phenylpyridines are typically used as ligands around the trivalent iridium ion to ensure a strong cyclometalation. The coordination sphere can be completed by more exotic heterocyclic structures in order to fine-tune the electronic properties of the corresponding cyclometalated phosphorescent emitters. Among those π-conjugated scaffolds surrounding the iridium(III) center, several examples can be found in the literature including 1,2,3-triazolylidene,[18] diisocyano-terphenyl,[19] N-heterocyclic carbene[20] or 2-(2-hydroxyphenyl) benzazole[21-23] (HBX) derivatives. HBX heterocycles have been extensively used as highly emissive fluorophores due to a beneficial excited-state intramolecular proton transfer (ESIPT) photophysical process, paving the way to many innovative applications.[24-25] Alternatively, they are excellent chelates for a wide range of metallic or metalloid ions.[26-28]

In this article, a series of cyclometalated iridium(III) complexes bearing a π -extended 2-(2-hydroxyphenyl) benzoxazole (HBO) ancillary ligand with terminal groups of different electronic nature (see Scheme 1) has been synthesized and their photophysical properties studied at room and low temperature. The nature of the transitions was probed in each case by TD-DFT calculations. Singlet oxygen sensitization studies were also performed for all complexes.

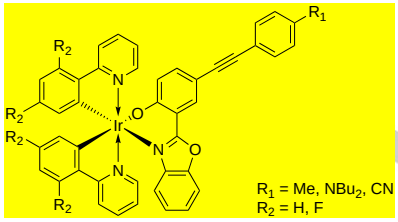

Scheme 1. General structure of complexes

Results and Discussion

Synthesis. The synthesis of the cyclometalated Iridium(III) complexes **4-6** and **7-9** is presented on Scheme 2. The synthetic targets can be obtained straightforwardly in one step, starting from the previously reported 2-(2'-hydroxyphenyl)benzoxazole (HBO) ligands **1-3**,[29] respectively functionalized by *p*-ethynyl-tolyl (R = Me), *p*-ethynyl-phenyl-N-dibutylamino (R = NBu_2) or *p*-ethynyl-benzonitrile (R = CN) groups. The formation of the targeted cyclometalated Iridium(III) complexes can be readily achieved by reacting the Iridium(III) chloro-bridged dimers precursors **A** or **B** with two equivalents of HBO chelates **1-3**, in the presence of an excess of potassium carbonate in a mixture of methanol and dichloromethane at 40 °C (Scheme 2). Pure Iridium(III) complexes were obtained in 47-72% yield after purification on a silica gel column chromatography. All dimers were characterized with ^{1}H-NMR spectroscopy and high-resolution mass spectrometry (HR-MS), reflecting their molecular structure in each case. Formation of the targeted complexes **4-6** and **7-9** was notably confirmed by assessing the disappearance of the downfield H-bonded phenolic proton present in the molecular structure of starting HBO ligands **1-3** by ^{1}H-NMR spectroscopy. All spectra can be found in the Supporting Information (SI). As reported for other similar Ir(III) cyclometalated complexes, it is expected that complexes **4-9** adopt a distorted octahedral geometry with the Nnitrogen atoms of the pyridine moiety in *trans* position.[30]

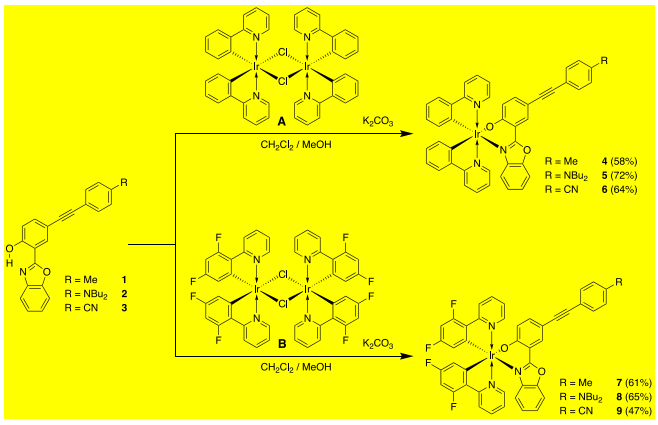

Scheme 2. Synthesis of cyclometalated Iridium(III) complexes **4-6** and **7-9**

Absorption. Absorption spectra of HBO ligands **1-3** and iridium(III) heteroleptic complexes **4-9**, recorded in acetonitrile solution at room temperature, are presented on Figure 1, while relevant main absorption parameters are listed in Table 1.

Ligands **1-3** display a strong absorption band centered around 330-340 nm with relatively high extinction coefficients (Figure 1). This band can be assigned to $^1\pi$-π^* transitions and its position and intensity is clearly affected by the nature of the substituent R (Scheme 2). In particular, the electron-withdrawing –CN and -donating –NBu_2 groups, both induce a blue-shift in the absorption of about 140 cm^{-1}, from 346 to 330 nm (Table 1). The HBO ligand **2**, functionalized with a NBu_2 moiety shows a second intense band at lower energy appearing as a shoulder.

All iridium(III) complexes **4-9** display an intense absorption band at about 250-260 nm (ε_{max} ~50-60,000 $M^{-1}\cdot cm^{-1}$) assigned by comparison to the archetypal [Ir(ppy)$_3$] complex to spin-allowed ^{1}LC transitions centered on the phenylpyridine ligands.[30] At lower energy, between 300 and 370 nm the complexes **4**, **5**, **7** and **8** are characterized by the presence of intense bands that, by comparison with the absorption spectra of the relevant HBO ligands **1** and **2**, can be attributed to spin allowed ligand centered (^{1}LC) transitions involving the HBO heterocycle. In complexes **6** and **9**, bearing the strong electron-withdrawing substituent –CN, these bands appear to be shifted at lower energy (λ_{max} = 371 and 364 nm, ε_{max} = 29,900 and 40,600 $M^{-1}\cdot cm^{-1}$, for **6** and **9**, respectively). The broad and moderately intense bands appearing above 380 nm and extending up to 450-500 nm (ε_{max} ~10,000 $M^{-1}\cdot cm^{-1}$) likely originate from iridium-based spin allowed metal-to-ligand charge transfer (^{1}MLCT) transitions, with possible weak contribution of formally spin forbidden triplet metal-to-ligand charge transfer (^{3}MLCT) transitions, induced by the presence of the heavy iridium center (ζ_{Ir} = 3,909 cm^{-1}).[31] It should be noted that only a limited effect on the absorption profiles and band positions is induced by the introduction of the fluorine atoms on the phenylpyridine rings. A more pronounced effect, especially on the bands observed between 300 and 370 nm, is induced by the substituents at the terminal position of the p-ethynylphenyl group (R = Me, CN or NBu_2).

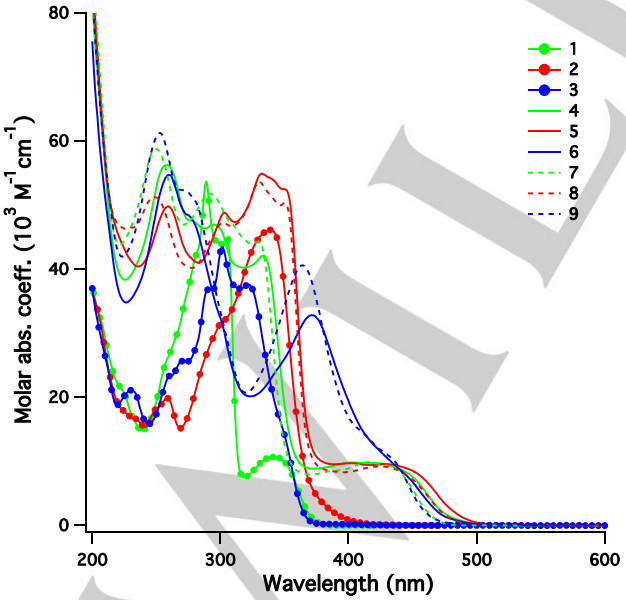

Figure 1. Absorption spectra of HBO ligands **1-3** and Iridium(III) complexes **4-9** in acetonitrile solution at rt.

Table 1. Absorption parameters

	λ, nm (ε, 10^3 $M^{-1}\cdot cm^{-1}$) [a]
1	281 sh (42.2), 289 (53.8), 305 (44.6), 342 (10.7)
2	258 (19.8), 302 sh (31.9), 339 (46.2)
3	230 (21.1), 261 sh (23.4), 271 (25.7), 291 (36.9), 302 (43.4), 322 (37.6), 350 sh (14.2)
4	258 (56.2), 295 (47.0), 333 (42.1), 420 (9.8)
5	259 (49.8), 303 (48.8), 332 (54.9), 350 (52.5), 430 (9.6)
6	260 (54.7), 274 sh (48.5), 371 (32.8), 435 (9.6)
7	250 (58.8), 292 (51.8), 330 (44.3), 415 (9.9)
8	249 (51.3), 302 (47.3), 330 (53.7), 350 (50.3), 425 (9.2)
9	253 (61.3), 270 sh (52.4), 364 (40.6), 430 (11.1)

[a] In acetonitrile solution at rt; sh is shoulder

Lowest-lying triplet states. Since iridium(III) complexes ultimately emit from excited states of triplet spin multiplicity, a TD-DFT investigation was performed to assess the energy and the nature of the lowest-lying triplet states of all the investigated complexes. The first four triplet excitations of compounds **4-9** are summarized in Figure 2 and described more in detail in SI in terms of Natural Transition Orbital (NTO) couples.[32] All the reported vertical excitations are computed at the ground-state minimum-energy geometry in acetonitrile, using the linear-response formalism.

Regardless of the complex, all the four lowest-energy triplets are essentially ^{3}LC states, with some minor contribution from the iridium *d* orbitals. For all compounds, the first two triplets (*i.e.*, T_1 and T_2) are centered on the benzoxazole-based ancillary ligand, while T_3 and T_4 mainly involve the two cyclometalating phenylpyridine ligands (see SI, Tables S4.1-6).

The substituents at the para position of the ethynyl-phenyl moiety of the ancillary ligand strongly affect the energy and the mutual position of the T_1 and T_2 states. In fact, although both triplet states are centered on the same ancillary ligand, only one of them has a pronounced charge-transfer (CT) nature, while the other is predominantly populated by a local excitation (LE). The CT state formally involves the promotion of one electron from the ethynyl-phenyl moiety of the ancillary ligand to the benzoxazole core. The energy of this CT state therefore strongly depends on the electronic nature of the terminal substituents attached to the ancillary ligand. On the other hand, the LE state is mainly a transition involving the π-π^* orbitals of the C≡C extended spacer of the ancillary ligand and the two nearby aromatic rings. LE states are less sensitive to the different electron-donating or -withdrawing substituents that are chemically attached to the ancillary ligand.

In the case of complexes **4** and **7**, functionalized with an innocent methyl group at the terminal position of the ancillary ligand, the lowest triplet (T_1) is the ^{3}LC-CT state, located 2.47–2.48 eV above S_0 in **4** and **7**, respectively. On the other hand, the ^{3}LC-LE state is 0.12 eV above T_1 in both cases. In complexes **5** and **8**, the presence of a strong electron donor substituent (NBu_2) leads to the stabilization of the ^{3}LC-CT state by 0.10–0.11 eV, as compared to **4** and **7**. The ^{3}LC-LE state also is stabilized, but only to a minor extent (0.02–0.03 eV). In the

case of complexes **6** and **9**, bearing a strong cyano acceptor, an increase of the energy of the ^{3}LC-CT state, in the range 0.10–0.11 eV is observed, with respect to the methyl-substituted complex **4** and **7**. Moreover, the cyano substituent is able to lower the energy of the π^* orbitals of the C≡C linker, owing to an increased electron delocalization, which triggers a stabilization of the corresponding ^{3}LC-LE state. As a consequence, a state flipping is observed and, for complexes **6** and **9**, the lowest triplet state is ^{3}LC-LE in nature, while the ^{3}LC-CT state is lifted to T_2.

As mentioned before, for all the complexes **4-9**, T_3 and T_4 are both mainly centered on the two cyclometalating ligands, which are nearly equivalent within each complex. As a consequence, these two triplets are almost degenerate and their energy is virtually affected only by the type of cyclometalating ligand. The presence or absence of fluorine on these ancillary ligands does not lead to any observable effects. The energy of T_3 and T_4 is calculated to be 2.67 ± 0.02 eV for the non-fluorinated complexes **4-6** and 2.82 ± 0.03 eV for the fluorinated complexes **7-9**. The energy increase observed in such transitions, by going from ppy to dfppy cyclometalating ligands, is a well-known effect, which is mainly ascribable to the stabilization of the highest-occupied π orbitals of the cyclometalating ligands, prompted by the electron-withdrawing fluorine atoms.[33-34]

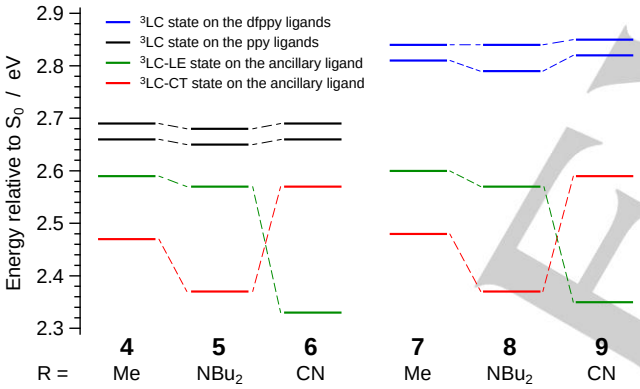

Figure 2. Energy diagram of the lowest-lying triplet states of complexes **4-9**, computed in acetonitrile as vertical excitations from the respective ground-state minimum-energy geometries. For further details see Tables S1–S6.

Emission. The luminescence emission properties analysis for the three ligands **1-3** and the six iridium(III) complexes **4-9** has been performed at room temperature in dilute acetonitrile solutions, in air-equilibrated and air-free conditions (Figure 3) and at low temperature in CH_2Cl_2:CH_3OH (1:1) glassy matrix. The relevant photophysical data are summarized in Table 2.

All ligands **1-3** and complexes **4-9** display an almost featureless broad spectrum in acetonitrile solution at room temperature. From the emission profiles, it is possible to identify some similarities in the optical behavior of the six investigated complexes. In particular, as previously observed in the absorption spectra (Figure 1), for complexes **5** and **8**, bearing a –NBu_2 group as substituent on the ancillary ligand, the emission profiles are the most red-shifted of the series. For the other complexes, the emission shapes and relative maxima are in the same range within the series of complexes with the same cyclometalating ligands, as for **4** and **6**, and for **7** and **9** (in this case, the second is just slightly blue-shifted than the former of ~7 nm). In all cases, the fluorinated derivatives **7-9** display a slightly blue-shifted emission wavelength with respect to the non-fluorinated congeners **4-6**.

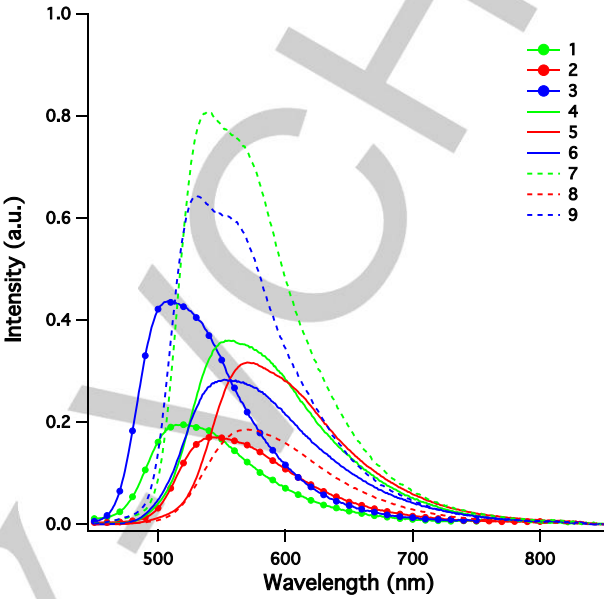

Figure 3. Emission spectra in de-aerated acetonitrile solution at room temperature of HBO ligands **1-3** and Iridium(III) complexes **4-9** in acetonitrile at room temperature. The area has been rescaled to the relevant quantum yield.

These results can be rationalized with the help of DFT calculations. In order to assess the nature of the emitting states, spin-unrestricted DFT calculations were carried out to optimize the lowest triplet state of all the complexes. After full geometry optimization, starting from the Franck-Condon region and imposing a spin multiplicity of 3, all complexes relax to a minimum that displays the same nature of the T_1 state computed by vertical excitations from the S_0 minimum (*i.e.*, no root-flipping is observed upon relaxation of T_1). As a consequence, a ^{3}LC-CT state is expected to be responsible for the emission of all complexes, with the notable exception of **6** and **9** (R = CN) which should emit from a ^{3}LC-LE state. The spin-density distributions of the lowest-energy triplet state of complexes **4-9** are reported in the SI (Figure S3.1) and their topologies can be compared to the NTO couples associated to the $S_0 \rightarrow T_1$ vertical transitions (SI, Tables S4.1-6).

In line with the experimental data, the emission of complexes **5** and **8** (R = NBu_2 group as substituent on the ancillary ligand) is estimated to occur at lower energy with respect to the other complexes (2.21 eV for **5** and **8**). These values compare well with the experimental data reported in Table 2 for room-temperature acetonitrile solutions (*i.e.*, 2.18 and 2.20 eV for **5** and **8**, respectively). Such a red-shifted emission is due the presence of the electron-donating amino substituent on the donor side of the ancillary ligand, which stabilizes the related ^{3}LC-CT emitting state.

On the other hand, the emission of **4** and **6** (R = Me and CN) is predicted to be very similar for both complexes and it is computed at (2.30 ± 0.02) eV. This is in line with experimental

data, despite the fact that the values are slightly overestimated when compared to emission spectra (*i.e.*, 2.23 and 2.24 eV for complexes **4** and **6**, respectively). This can be easily justified considering that the DFT estimated emission is computed as an adiabatic energy difference between S_0 and T_1. As for the fluorinated analogues **7** and **9**, a minor blue shift in the emission energy is also expected from the calculations, despite the theoretical shift being underestimated compared to the experimental data (*i.e.*, 0.03 *vs.* 0.09 eV).

It is worth stressing that, although complexes **4** and **6** (and the fluorinated analogues **7** and **9**) display almost identical luminescence profiles and energies, they actually emit from triplet excited states of different nature (*i.e.*, a ^{3}LC-CT state for **4** and **7** and a ^{3}LC-LE state for **6** and **9**). The fact that the emission energy of these complexes is very similar is just a coincidence.

All complexes display bright emission both at room and at low temperature. The ~~PLQY values~~ emission quantum yield (ϕ) of **4-9** ranges from 0.11 to 0.44, in de-aerated acetonitrile solutions. Moreover, the fluorinated derivatives **7-9** display the highest values of lifetimes and k_r in the series (Table 2). As denoted by the calculated values of the radiative constants for all the complexes ($k_r = \phi / \tau$, values from 1.2 to 6.9×10^4 s^{-1}), are one order of magnitude lower than those of reported iridium(III) complexes, emitting from a state with an important ligand-centered contribution.[30]

Table 2. Emission parameters

	rt [a]			77 K [b]	
	λ_{em}, nm	ϕ	τ, µs (~~k_r s^{-1}~~)	λ_{em}, nm	τ, µs
1	517	0.11 (4.81×10^{-2})			
2	546	0.10 (0.75×10^{-2})			
3	514	0.22 (8.20×10^{-2})			
4	555	0.22 (0.33×10^{-2})	3.2 (42.0×10^{-3})	513	7.5
5	568	0.19 (0.14×10^{-2})	5.8 (36.4×10^{-3})	527	13.8
6	554	0.18 (0.24×10^{-2})	2.9 (40.8×10^{-3})	513	190
7	537	0.44 (0.17×10^{-2})	12.7 (50.9×10^{-3})	502	14.3
8	563	0.11 (0.08×10^{-2})	9.2 (43.5×10^{-3})	525	27.6
9	530	0.35 (0.09×10^{-2})	19.1 (56.5×10^{-3})	509	420

[a] Quantum yield and lifetime values in de-aerated (and air-equilibrated) acetonitrile solution; λ_{exc} = 420 nm and 370 nm for quantum yield and lifetime measurements, respectively. [b] In DCM:MeOH (1:1) glassy solution, λ_{exc} = 400 nm and 370 nm for spectra and lifetime measurements.

All these evaluations and comparisons with theoretical data reveal the suitability of this kind of complexes whose photophysical properties can be efficiently modified through mild structural alteration. The color coordinates in the CIE 1931 color space have been calculated for the different HBO ligands **1-3** and Iridium(III) complexes **4-9** from the relevant irradiance spectra. The results are compared in Figure 4. It should be observed that the emission color of the iridium complexes can be finely tuned, by simply changing the nature of substituent on the ppy and HBO ligands, from yellow (**5**: 0.499, 0.493) to yellow green (**9**: 0.389, 0.578). The HBO ligands **1** and **3** afford a yellowish green color (*ca.* 0.29, 0.55).

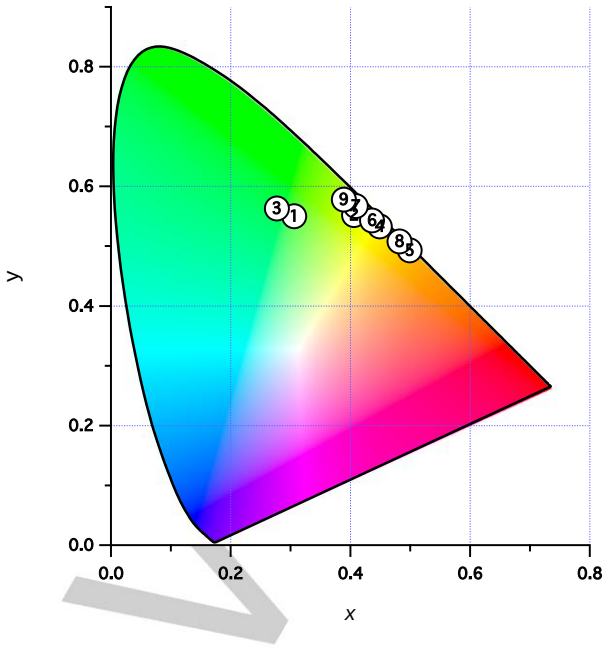

Figure 4. CIE 1931 spectral chromaticity coordinates of **1-9** in CH_3CN at rt.

In glassy matrix at 77 K, the iridium(III) complexes **5** and **8** (R = NBu_2) display red-shifted emissions, as compared to the other complexes in the series bearing the same cyclometalating ligands (Figure 5). This feature was already observed on the maximum emission wavelength at room-temperature acetonitrile spectra.

For all Iridium(III) complexes, a pronounced structuration of the emission bands is observed at low temperature, revealing a fine vibronic progression, further indicating a strongly ligand-centered nature of the emitting states (Figure 5). This experimental observation strongly supports the ^{3}LC attribution to the nature of the lowest-lying triplet states. In addition, the high blue shift of the emission profiles recorded at 77 K, with respect to those obtained at room temperature, clearly suggests the involvement of transitions with a high charge-transfer character (rigidochromic effect). These findings are in line with the presence of ^{3}LC-CT emitting states, as indicated by DFT calculations. It is also worth-mentioning that the excited-state lifetimes of **6** and **9** (R = CN) at 77 K are more than ten times longer with respect of those of the other investigated complexes (R = Me, NBu_2). This does indicate that, for the cyano-substituted complexes **6** and **9**, the nature of the emitting state is different from that of the other Iridium(III) complexes **4**,**5** and **7**,**8**. Again, this experimental observation is in line with DFT predictions, which estimate the ^{3}LC-LE to be lower in energy with respect to the ^{3}LC-CT state, only for complexes **6** and **9**.

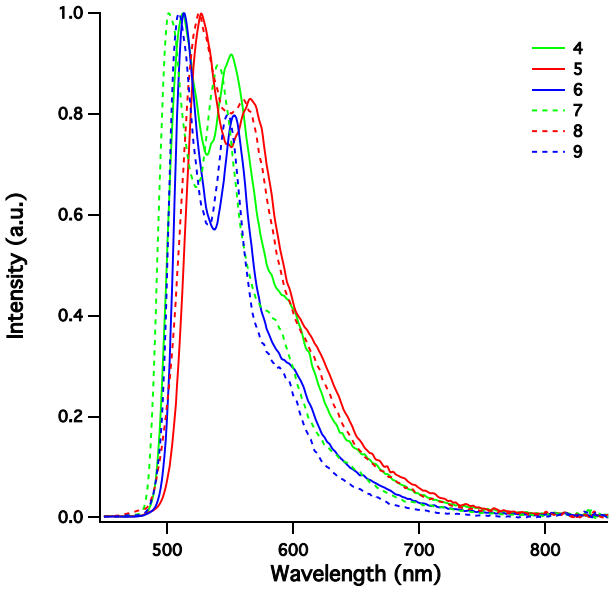

Figure 5. Normalized emission spectra in DCM:MeOH 1:1 (v/v) mixture at 77 K.

Singlet Oxygen sensitization. All the complexes show a strong reduction of luminescence quantum yield in air-equilibrated solution (Table 2); a feature commonly observed for iridium(III) complexes. This indicates the occurrence of a triplet-triplet energy transfer to molecular oxygen, generating the $^1O_2$ ($^1\Delta_g$) excited species. The process can be schematized as follow:

$$P \xrightarrow{h\nu} {}^1P^* \xrightarrow{ISC} {}^3P^* \xrightarrow{O_2} P + {}^1O_2^*$$

where P is the photosensitizer (*i.e.*, the Iridium(III) complexes **4-9**), $^1P^*$ and $^3P^*$ are the lowest-lying singlet and triplet excited states and ISC stands for intersystem crossing.

The bimolecular rate constant of the sensitization process, k_q, can be determined from the excited-state lifetimes in air-equilibrated (τ_q) and O_2-free (τ_0) solutions by means of the Stern-Volmer equation:[35]

$$\tau_q^{-1} = \tau_0^{-1} + k_q[O_2]$$

in which $[O_2]$ is the oxygen concentration.

By substituting the relevant lifetime values reported in Table 2, one obtains k_q ~1×10^{10} $M^{-1}s^{-1}$ for all complexes **4-9** (Table 3). This is close to the diffusional limit of the quenching rate constant in acetonitrile (k_{diff} = 1.9×10^{10} $M^{-1}s^{-1}$),[31] as often observed for iridium(III) complexes.[30]

The quantum yields of sensitization of singlet oxygen (ϕ_Δ) can be determined by comparison between the typical luminescence centered at 1280 nm of iso-absorbing (λ_{exc} = 442 nm) methanol solutions of complexes **4-9**, and $[Ru(bpy)_3]^{2+}$ in the same solvent (ϕ_Δ = 0.90). The values obtained for ϕ_Δ are reported in Table 3 and the luminescence spectra of $^1O_2$ are shown in Figure 6. The complexes **6** and **9**, bearing the –CN terminal substituent ~~and also showing the longest excited state lifetime in the series~~, display the highest quantum yield of sensitization. They are therefore, capable of combining an extremely fast reaction rate with a still very high yield of production of the reactive singlet oxygen species (70-74%, Table 3). This interesting feature make them very attractive candidates for photodynamic therapy applications.[36] The other complexes (*i.e.*, **4**, **5**, **7** and **8**,) although maintaining reaction rates close to the diffusional limit, have lower quantum yield, on the order of 50% (Table 3).

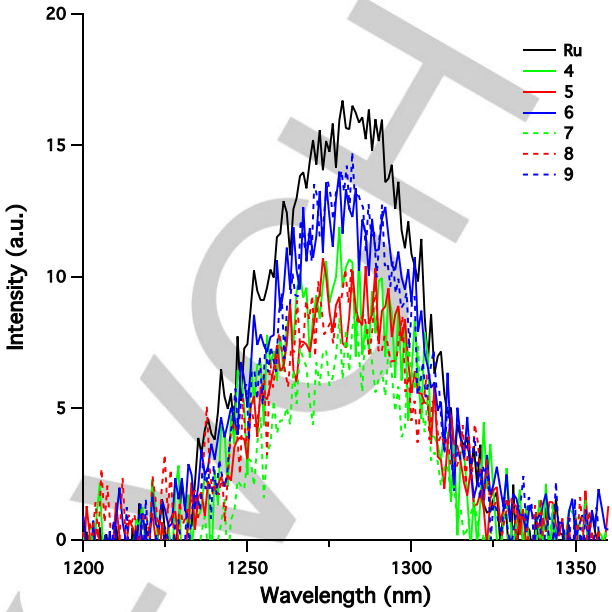

Figure 6. Emission spectra of $^1O_2$ in air-equilibrated methanol solutions for Iridium(III) complexes **4-9** (**Ru** is $[Ru(bpy)_3]^{2+}$); the area has been rescaled to the relevant quantum yield of sensitization.

Table 3. Singlet oxygen ($^1\Delta_g$) sensitization parameters

	k_q (M^{-1} s^{-1}) [a]	ϕ_Δ [b]
4	1.2×10^{10}	0.49
5	1.4×10^{10}	0.53
6	1.3×10^{10}	0.74
7	1.0×10^{10}	0.37
8	1.2×10^{10}	0.54
9	0.9×10^{10}	0.70

[a] In air-equilibrated methanol solution at room temperature. [b] Calculated with respect to $[Ru(bpy)_3]^{2+}$ in air-equilibrated methanol solution (ϕ_Δ = 0.90).[37]

Conclusion

A series of six cyclometalated iridium(III) complexes containing a functionalized HBO-based N^O chelate have been synthesized and their photophysical properties fully studied at room and low temperature, in air-equilibrated or de-aerated conditions. These complexes exhibit bright phosphorescence and a fine-tuning of their emission color can be achieved by simply modifying the terminal group of the ancillary ligand. DFT calculations indicate that all the complexes emit from a ligand-centered excited-state involving the HBO ancillary ligand. Anyway, the terminal group on this ligand has a huge impact on the nature of the emitting state: an internal charge-transfer transition is responsible for emission in the case of electron-donating groups (such as Me

and NBu_2), while a locally-excited state becomes active, when the ancillary ligand is equipped with an electron-withdrawing cyano substituent. This difference in the emission nature is further corroborated by the longer excited-state lifetimes observed in glassy matrix at low temperature for the complexes having the electron-withdrawing CN terminal group. Finally, these iridium(III) complexes display competitive singlet oxygen sensitization parameters making them attractive candidates as sensitizers in photodynamic therapy. Work along these lines is currently in progress.

Experimental Section

Materials and Methods. All reactions were performed under a dry atmosphere of argon. Chemicals were purchased from commercial sources and used without further purification. Reaction solvents were distilled according to common procedures. Thin layer chromatography (TLC) was performed on silica gel or aluminum oxide plates coated with fluorescent indicator. Chromatographic purifications were conducted using 40-63 µm silica gel. All mixtures of solvents are given in v/v ratio. ^{1}H-NMR (400.1 MHz) spectra were recorded on a Bruker Advance 400 MHz spectrometer with perdeuterated solvents containing residual protonated solvent signals as internal references. The cyclometalated Iridium(III) chloro-bridged dimers **A**[38] and **B**[38] and the ethynyl-extended 2-(2'-hydroxyphenyl) benzoxazole ligands **1-3**[29] were synthesized according to reported procedures.

General procedure. In a Schlenk tube, under an inert atmosphere, the cyclometalated Iridium(III) chloro-bridged dimer **A** or **B** (0.1 mmol) and potassium carbonate (2 mmol) were dissolved in a mixture of CH_2Cl_2/CH_3OH (1:1, v:v). 5-extended-2-2'(hydroxyphenyl)benzoxazole) **1-3** (0.2 mmol) were then added to the resulting suspensions and the mixtures were subsequently stirred for 24 hours at 40 °C. After cooling down, the crude mixtures were extracted with CH_2Cl_2, washed with water, dried ($MgSO_4$), and the solvents removed *in vacuo*. The crude residues were purified by column chromatography on SiO_2 eluting with CH_2Cl_2/pet. ether to yield complexes **4-9** as yellow powders in 47-72% yield.

Complex 4: yellow powder. 58%. ^{1}H-NMR (400 MHz, $CDCl_3$) δ (ppm) = 8.74 (d, 1H, CH Ar, *J* = 5.2 Hz), 8.14 (d, 1H, CH Ar, *J* = 2.4 Hz), 8.02 (d, 1H, CH Ar, *J* = 5.6 Hz), 7.79 (d, 1H, CH Ar, *J* = 8 Hz), 7.72 (d, 1H, CH Ar, *J* = 8 Hz), 7.51-7.60 (m, 4H, CH Ar), 7.37 (d, 1H, CH Ar, *J* = 8 Hz), 7.32 (d, 2H, CH Ar, *J* = 8 Hz), 7.23 (dd, 1H, CH Ar, *J* = 9 Hz), 7.05-7.08 (m, 3H, CH Ar), 6.97 (t, 1H, CH Ar, *J* = 6 Hz), 6.68-6.87 (m, 6H, CH Ar), 6.62 (d, 1H, CH Ar, *J* = 9.2 Hz), 6.40 (d, 1H, CH Ar, *J* = 7.6 Hz), 6.11 (d, 1H, CH Ar, *J* = 7.6 Hz), 6.01 (d, 1H, CH Ar, *J* = 8.4 Hz), 2.28 (s, 3H, CH_3). ESI-HRMS: calcd for $C_{44}H_{31}IrN_3O_2$ (M+H) 826.2043, found (M+H) 826.2052.

Complex 5: Yellow powder. 72%. ^{1}H-NMR (400 MHz, $CDCl_3$) δ (ppm) = 8.74 (d, 1H, CH Ar, *J* = 5.6 Hz), 8.19 (d, 1H, CH Ar, *J* = 2.4 Hz), 8.10 (d, 1H, CH Ar, *J* = 6 Hz), 7.84 (d, 1H, CH Ar, *J* = 8 Hz), 7.77 (d, 1H, CH Ar, *J* = 8 Hz), 7.56-7.64 (m, 4H, CH Ar), 7.44 (d, 1H, CH Ar, *J* = 8 Hz), 7.29-7.35 (m, 3H, CH Ar), 7.12 (t, 1H, CH Ar, *J* = 8 Hz), 7.03 (t, 1H, CH Ar, *J* = 6.4 Hz), 6.75-6.94 (m, 6H, CH Ar), 6.69 (d, 1H, CH Ar, *J* = 8.8 Hz), 6.57 (d, 2H, CH Ar, *J* = 8.8 Hz), 6.48 (d, 1H, CH Ar, *J* = 8.4 Hz), 6.19 (d, 1H, CH Ar, *J* = 7.2 Hz), 6.09 (d, 1H, CH Ar, *J* = 8.4 Hz), 3.28 (t, 4H, CH_2, *J* = 7.6 Hz), 1.54-1.62 (m, 4H, CH_2), 1.32-1.41 (m, 4H, CH_2), 0.97 (t, 6H, CH_3, *J* = 7.2 Hz). ESI-HRMS: calcd for $C_{51}H_{46}IrN_4O_2$ (M+H) 939.3248, found (M+H) 939.3230.

Complex 6: Yellow powder. 64%. ^{1}H-NMR (400 MHz, $CDCl_3$) δ (ppm) = 8.78 (d, 1H, CH Ar, *J* = 5.6 Hz), 8.25 (d, 1H, CH Ar, *J* = 2 Hz), 8.08 (d, 1H, CH Ar, *J* = 5.2 Hz), 7.87 (d, 1H, CH Ar, *J* = 8 Hz), 7.79 (d, 1H, CH Ar, *J* = 8.4 Hz), 7.59-7.68 (m, 6H, CH Ar), 7.53 (d, 2H, CH Ar, *J* = 8.4 Hz), 7.46 (d, 1H, CH Ar, *J* = 8.4 Hz), 7.31 (dd, 1H, CH Ar, *J* = 8 Hz), 7.15 (t, 1H, CH Ar, *J* = 7.6 Hz), 7.05 (t, 1H, CH Ar, *J* = 6.4 Hz), 6.76-6.96 (m, 6H, CH Ar), 6.71 (d, 1H, CH Ar, *J* = 8.8 Hz), 6.46 (d, 1H, CH Ar, *J* = 7.6 Hz), 6.18 (d, 1H, CH Ar, *J* = 7.6 Hz), 6.09 (d, 1H, CH Ar, *J* = 8.4 Hz). ESI-HRMS: calcd for $C_{44}H_{27}IrN_4O_2$ (M+) 836.1760, found (M+) 836.1730.

Complex 7: Yellow powder. 61%. ^{1}H-NMR (400 MHz, $CDCl_3$) δ (ppm) = 8.77 (d, 1H, CH Ar, *J* = 6 Hz), 8.28 (d, 1H, CH Ar, *J* = 8.8 Hz), 8.19-8.22 (m, 2H, CH Ar), 7.08 (d, 1H, CH Ar, *J* = 6 Hz), 7.71 (q, 2H, CH Ar, *J* = 7.2 Hz), 7.49 (d, 1H, CH Ar, *J* = 8 Hz), 7.40 (d, 2H, CH Ar, *J* = 8 Hz), 7.34 (dd, 1H, CH Ar, *J* = 9.2 Hz), 7.20 (t, 1H, CH Ar, *J* = 8 Hz), 7.08-7.15 (m, 3H, CH Ar), 6.91-6.97 (m, 2H, CH Ar), 6.71 (d, 1H, CH Ar, *J* = 8.8 Hz), 6.38-6.51 (m, 2H, CH Ar), 6.22 (d, 1H, CH Ar, *J* = 8 Hz), 5.92 (dd, 1H, CH Ar, *J* = 8.8 Hz), 5.57 (dd, 1H, CH Ar, *J* = 8.2 Hz), 2.36 (s, 3H, CH_3). ESI-HRMS: calcd for $C_{44}H_{26}F_4IrN_3O_2$ (M+) 897.1588, found (M+) 897.1611.

Complex 8: Yellow powder. 65%. ^{1}H-NMR (400 MHz, $CDCl_3$) δ (ppm) = 8.70 (d, 1H, CH Ar, *J* = 6 Hz), 8.21 (d, 1H, CH Ar, *J* = 8.4 Hz), 8.09-8.14 (m, 2H, CH Ar), 8.01 (d, 1H, CH Ar, *J* = 8 Hz), 7.61-7.67 (m, 2H, CH Ar), 7.41 (d, 1H, CH Ar, *J* = 8 Hz), 7.23-7.26 (m, 3H, CH Ar), 7.12 (t, 1H, CH Ar, *J* = 8.4 Hz), 7.02 (t, 1H, CH Ar, *J* = 7.2 Hz), 6.83-6.88 (m, 2H, CH Ar), 6.61 (d, 1H, CH Ar, *J* = 8.8 Hz), 6.50 (d, 2H, CH Ar, *J* = 8 Hz), 6.30-6.43 (m, 2H, CH Ar), 6.13 (d, 1H, CH Ar, *J* = 8 Hz), 5.84 (d, 1H, CH Ar, *J* = 8.8 Hz), 5.49 (d, 1H, CH Ar, *J* = 8.4 Hz), 3.20 (t, 4H, CH2, *J* = 6.4 Hz), 1.46-1.54 (m, 4H, CH_2), 1.24-1.33 (m, 4H, CH_2), 0.89 (t, 6H, CH_3, *J* = 7.6 Hz). ESI-HRMS: calcd for $C_{51}H_{42}F_4IrN_4O_2$ (M+H) 1011.2871, found (M+H) 1011.2907.

Complex 9: Yellow powder. 47%. ^{1}H-NMR (400 MHz, $CDCl_3$) δ (ppm) = 8.73 (d, 1H, CH Ar, *J* = 6 Hz), 8.30 (d, 1H, CH Ar, *J* = 8 Hz), 8.20-8.24 (m, 2H, CH Ar), 8.06 (d, 1H, CH Ar, *J* = 5.6 Hz), 7.70-7.76 (m, 2H, CH Ar), 7.49-7.61 (m, 5H, CH Ar), 7.34 (dd, 1H, CH Ar, *J* = 8.8 Hz), 7.22 (t, 1H, CH Ar, *J* = 7.6 Hz), 7.10 (t, 1H, CH Ar, *J* = 6.4 Hz), 6.95 (q, 2H, CH Ar, *J* = 7.2 Hz), 6.72 (d, 1H, CH Ar, *J* = 8.8 Hz), 6.39-6.52 (m, 2H, CH Ar), 6.21 (d, 1H, CH Ar, *J* = 8.4 Hz), 5.90 (d, 1H, CH Ar, *J* = 8.4 Hz), 5.56 (d, 1H, CH Ar, *J* = 8.4 Hz). ESI-HRMS: calcd for $C_{44}H_{24}F_4IrN_4O_2$ (M+H) 909.1462, found (M+H) 909.1491.

Photophysics. Absorption spectra of dilute acetonitrile (VWR Uvasol) solutions were recorded on a Perkin Elmer Lambda 950 UV/Vis/NIR spectrophotometer. The molar absorption coefficients were calculated by applying the Lambert-Beer law to low absorbance spectra (A < 1) recorded at successive dilutions. Steady-state photoluminescence spectra were measured on an Edinburgh FLS920 Vis/NIR fluorimeter, equipped with a Hamamatsu R928P Peltier-cooled (Vis) and a super-cooled (193 K) Hamamatsu R5509-72 (NIR) PMTs. The concentration of sample solutions was adjusted to obtain absorption values A < 0.1 at the excitation wavelength and the solutions de-aerated by bubbling Ar for at least 20 minutes. The correction curve of the wavelength dependent phototube response between 280 and 1600 nm has been obtained by using a calibrated deuterium / halogen lamp source DH-3*plus*-CAL-EXT (Ocean Optics). Luminescence quantum efficiencies in solution were evaluated with reference to quinine sulfate (ϕ = 0.53, in air-equilibrated 0.1 N H_2SO_4).[31] Band maxima and quantum yields were obtained with uncertainty of 2 nm and 20%, respectively. Luminescence lifetimes were measured with an IBH 5000F time-correlated single-photon counting (TCSPC) device, by using pulsed NanoLED and SpectraLED excitation sources at 331 and 370 nm. The analysis of the luminescence decay profiles against time was accomplished with the DAS6 Fluorescence Decay Analysis Software (Horiba). Experimental uncertainties in the lifetime determinations are estimated to be 10%. Singlet oxygen sensitization efficiencies have been measured with reference to $[Ru(bpy)_3]^{2+}$ in CH_3OH (ϕ_Δ = 0.90)[37] by comparing the area of singlet oxygen phosphorescence spectra. Excitation at 442 nm has been performed with a HeCd laser (Kimmon).

DFT Calculations. Density functional theory (DFT) calculations were carried out using the D.01 revision of the Gaussian 09 program package[39] in combination with the M06 global-hybrid meta-GGA

exchange-correlation functional.[40-41] The fully relativistic Stuttgart/Cologne energy-consistent pseudopotential with multielectron fit was used to replace the first 60 inner-core electrons of the iridium metal center (*i.e.*, ECP60MDF) and was combined with the associated triple-ζ basis set (*i.e.*, cc-pVTZ-PP basis);[42] for all other atoms, the Pople 6-31G(d,p) basis set was adopted.[43] All the reported complexes were fully optimized without symmetry constraints, using a time-independent DFT approach, in their ground state (S_0) and triplet emitting state (T_1). All the optimization procedures were performed using the polarizable continuum model (PCM) to simulate acetonitrile solvation effects.[44-46] Frequency calculations were always used to confirm that every stationary point found by geometry optimizations was actually a minimum on their corresponding potential-energy surfaces (no imaginary frequencies). To investigate the nature of the emitting states, geometry optimizations and frequency calculations were performed at the spin-unrestricted UM06 level of theory (imposing a spin multiplicity of 3), using the corresponding S_0 minimum-energy geometry as starting point. The emission energy from the lowest triplet excited state was estimated by subtracting the SCF energy of the emitting state (T_1) from that of the singlet ground state (S_0), both in their minimum-energy conformation (adiabatic energy difference). Time-dependent DFT calculations (TD-DFT),[47-49] carried out at the same level of theory used for geometry optimizations, were used to locate the lowest-energy 12 vertical excitations of triplet spin multiplicity, starting from the ground-state minimum-energy geometry of each complex. The nature of the transitions was assessed by the help of Natural Transition Orbital (NTO) analysis.[32] All the pictures showing molecular geometries, orbitals and spin-density surfaces were created using GaussView 6.[50]

Acknowledgements

J.M and G.U. are grateful to the Centre National de la Recherche Scientifique (CNRS) for providing research facilities and the Agence Nationale de la Recherche (ANR project GeDeMi) for financial support. Funding from the Italian CNR (project PHEEL) is also acknowledged.

Keywords: Iridium complexes • Hydroxybenzazoles • Luminescence • Phosphorescence • Charge Transfer Excited State

[1] X. W. Chen, J. L. Liao, Y. M. Liang, M. O. Ahmed, H. E. Tseng, S. A. Chen, *J. Am. Chem. Soc.* **2003**, *125*, 636-637.
[2] X. Y. Du, S. L. Tao, Y. Huang, X. X. Yang, X. L. Ding, X. H. Zhang, *Appl. Phys. Lett.* **2015**, *107*, 1833041-1833045.
[3] X. Y. Du, J. W. Zhao, S. L. Yuan, C. J. Zheng, H. Lin, S. L. Tao, C. S. Lee, *J. Mater. Chem. C* **2016**, *4*, 5907-5913.
[4] J. P. Duan, P. P. Sun, C. H. Cheng, *Adv. Mater.* **2003**, *15*, 224-228.
[5] C. Wu, S. L. Tao, M. M. Chen, F. L. Wong, Y. Yuan, H. W. Mo, W. M. Zhao, C. S. Lee, *Chem.-Asian J.* **2013**, *8*, 2575-2578.
[6] J. Massue, J. Olesiak-Banska, E. Jeanneau, C. Aronica, K. Matczyszyn, M. Samoc, C. Monnereau, C. Andraud, *Inorg. Chem.* **2013**, *52*, 10705-10707.
[7] H. L. Chen, Q. Zhao, Y. B. Wu, F. Y. Li, H. Yang, T. Yi, C. H. Huang, *Inorg. Chem.* **2007**, *46*, 11075-11081.
[8] Y. Liu, M. Y. Li, Q. Zhao, H. Z. Wu, K. W. Huang, F. Y. Li, *Inorg. Chem.* **2011**, *50*, 5969-5977.
[9] H. F. Shi, S. J. Liu, H. B. Sun, W. J. Xu, Z. F. An, J. A. Chen, S. Sun, X. M. Lu, Q. A. Zhao, W. Huang, *Chem.-Eur. J.* **2010**, *16*, 12158-12167.
[10] D. R. Whang, Y. You, W. S. Chae, J. Heo, S. Kim, S. Y. Park, *Langmuir* **2012**, *28*, 15433-15437.
[11] K. K. W. Lo, *Acc. Chem. Res.* **2015**, *48*, 2985-2995.
[12] K. K. W. Lo, K. H. K. Tsang, K. S. Sze, C. K. Chung, T. K. M. Lee, K. Y. Zhang, W. K. Hui, C. K. Li, J. S. Y. Lau, D. C. M. Ng, N. Zhu, *Coord. Chem. Rev.* **2007**, *251*, 2292-2310.
[13] D. L. Ma, W. L. Wong, W. H. Chung, F. Y. Chan, P. K. So, T. S. Lai, Z. Y. Zhou, Y. C. Leung, K. Y. Wong, *Angew. Chem. Int. Ed.* **2008**, *47*, 3735-3739.
[14] C. J. Chang, C. H. Yang, K. Chen, Y. Chi, C. F. Shu, M. L. Ho, Y. S. Yeh, P. T. Chou, *Dalton Trans.* **2007**, 1881-1890.
[15] L. Guang, *J. Lumin.* **2011**, *131*, 184-189.
[16] G. N. Li, C. W. Gao, H. H. Chen, T. T. Chen, H. Xie, S. Lin, W. Sun, G. Y. Chen, Z. G. Niu, *Inorg. Chim. Acta* **2016**, *445*, 22-27.
[17] X. Qin, M. Li, M. Xiang, Y. Luo, Y. Jiao, R. Yuan, N. Wang, Z. Lu, X. Pu, *ChemPhysChem* **2019**, *20*, 470-481.
[18] A. Baschieri, F. Monti, E. Matteucci, A. Mazzanti, A. Barbieri, N. Armaroli, L. Sambri, *Inorg. Chem.* **2016**, *55*, 7912-7919.
[19] F. Monti, A. Baschieri, E. Matteucci, A. Mazzanti, L. Sambri, A. Barbieri, N. Armaroli, *Faraday Discuss.* **2015**, *185*, 233-248.
[20] P. H. Lanoe, J. Chan, G. Gontard, F. Monti, N. Armaroli, A. Barbieri, H. Amouri, *Eur. J. Inorg. Chem.* **2016**, 1631-1634.
[21] Y. Y. Hao, X. X. Guo, L. P. Lei, J. N. Yu, H. X. Xu, B. S. Xu, *Synth. Met.* **2010**, *160*, 1210-1215.
[22] H. R. Park, Y. Ha, *Mol. Cryst. Liq. Cryst.* **2012**, *567*, 149-155.
[23] Y. You, J. Seo, S. H. Kim, K. S. Kim, T. K. Ahn, D. Kim, S. Y. Park, *Inorg. Chem.* **2008**, *47*, 1476-1487.
[24] K. Benelhadj, W. Muzuzu, J. Massue, P. Retailleau, A. Charaf-Eddin, A. D. Laurent, D. Jacquemin, G. Ulrich, R. Ziessel, *Chem.-Eur. J.* **2014**, *20*, 12843-12857.
[25] J. Massue, A. Felouat, M. Curtil, P. M. Vérité, D. Jacquemin, G. Ulrich, *Dyes Pigm.* **2019**, *160*, 915-922.
[26] J. Cerezo, A. Requena, J. Zuniga, M. J. Piernas, M. D. Santana, J. Perez, L. Garcia, *Inorg. Chem.* **2017**, *56*, 3663-3673.
[27] M. A. Katkova, T. V. Balashova, V. A. Ilichev, A. N. Konev, N. A. Isachenkov, G. K. Fukin, S. Y. Ketkov, M. N. Bochkarev, *Inorg. Chem.* **2010**, *49*, 5094-5100.
[28] J. Massue, D. Frath, G. Ulrich, P. Retailleau, R. Ziessel, *Org. Lett.* **2012**, *14*, 230-233.
[29] J. Massue, D. Frath, P. Retailleau, G. Ulrich, R. Ziessel, *Chem.-Eur. J.* **2013**, *19*, 5375-5386.
[30] L. Flamigni, A. Barbieri, C. Sabatini, B. Ventura, F. Barigelletti, in *Photochemistry and Photophysics of Coordination Compounds Ii, Vol. 281* (Eds.: V. Balzani, S. Campagna), **2007**, pp. 143-203.
[31] M. Montalti, A. Credi, L. Prodi, M. T. Gandolfi, *Handbook of Photochemistry*, 3rd ed., CRC Press, Boca Raton, FL, **2006**.
[32] R. L. Martin, *J. Chem. Phys.* **2003**, *118*, 4775-4777.
[33] E. C. Constable, M. Neuburger, P. Rosel, G. E. Schneider, J. A. Zampese, C. E. Housecroft, F. Monti, N. Armaroli, R. D. Costa, E. Orti, *Inorg. Chem.* **2013**, *52*, 885-897.
[34] R. D. Costa, E. Orti, H. J. Bolink, F. Monti, G. Accorsi, N. Armaroli, *Angew. Chem. Int. Ed.* **2012**, *51*, 8178-8211.
[35] J. R. Lakowicz, *Principles of Fluorescence Spectroscopy*, 3rd ed., Springer US, **2006**.
[36] L. K. McKenzie, I. V. Sazanovich, E. Baggaley, M. Bonneau, V. Guerchais, J. A. G. Williams, J. A. Weinstein, H. E. Bryant, *Chem.-Eur. J.* **2017**, *23*, 234-238.
[37] F. Wilkinson, W. P. Helman, A. B. Ross, *J. Phys. Chem. Ref. Data* **1993**, *22*, 113-262.
[38] M. Nonoyama, *Bull. Chem. Soc. Jpn.* **1974**, *47*, 767-768.
[39] M. J. Frisch, G. W. Trucks, H. B. Schlegel, G. E. Scuseria, M. A. Robb, J. R. Cheeseman, G. Scalmani, V. Barone, B. Mennucci, G. A. Petersson, H. Nakatsuji, M. Caricato, X. Li, H. P. Hratchian, A. F. Izmaylov, J. Bloino, G. Zheng, J. L. Sonnenberg, M. Hada, M. Ehara, K. Toyota, R. Fukuda, J. Hasegawa, M. Ishida, T. Nakajima, Y. Honda, O. Kitao, H. Nakai, T. Vreven, J. A. Montgomery Jr., J. E. Peralta, F. Ogliaro, M. Bearpark, J. J. Heyd, E. Brothers, K. N. Kudin, V. N. Staroverov, R. Kobayashi, J. Normand, K. Raghavachari, A. Rendell, J. C. Burant, S. S. Iyengar, J. Tomasi, M. Cossi, N. Rega, J. M. Millam, M. Klene, J. E. Knox, J. B. Cross, V. Bakken, C. Adamo, J. Jaramillo, R. Gomperts, R. E. Stratmann, O. Yazyev, A. J. Austin, R. Cammi, C. Pomelli, J. W. Ochterski, R. L. Martin, K. Morokuma, V. G. Zakrzewski, G. A. Voth, P. Salvador, J. J. Dannenberg, S. Dapprich, A. D. Daniels, O. Farkas, J. B. Foresman, J. V. Ortiz, J. Cioslowski, D. J. Fox, *Gaussian 09, Revision D.01*, Gaussian, Inc., Wallingford CT, **2009**
[40] Y. Zhao, D. G. Truhlar, *Theor. Chem. Acc.* **2008**, *120*, 215-241.

[41] Y. Zhao, D. G. Truhlar, *Acc. Chem. Res.* **2008**, *41*, 157-167.
[42] D. Figgen, K. A. Peterson, M. Dolg, H. Stoll, *J. Chem. Phys.* **2009**, *130*, 164108.
[43] G. A. Petersson, A. Bennett, T. G. Tensfeldt, M. A. Al‐Laham, W. A. Shirley, J. Mantzaris, *J. Chem. Phys.* **1988**, *89*, 2193-2218.
[44] C. J. Cramer, D. G. Truhlar, in *Solvent Effects and Chemical Reactivity, Vol. 17* (Eds.: O. Tapia, J. Bertrán), Springer Netherlands, **2002**, pp. 1-80.
[45] J. Tomasi, B. Mennucci, R. Cammi, *Chem. Rev.* **2005**, *105*, 2999-3093.
[46] J. Tomasi, M. Persico, *Chem. Rev.* **1994**, *94*, 2027-2094.
[47] R. Bauernschmitt, R. Ahlrichs, *Chem. Phys. Lett.* **1996**, *256*, 454-464.
[48] M. E. Casida, C. Jamorski, K. C. Casida, D. R. Salahub, *J. Chem. Phys.* **1998**, *108*, 4439-4449.
[49] R. E. Stratmann, G. E. Scuseria, M. J. Frisch, *J. Chem. Phys.* **1998**, *109*, 8218-8224.
[50] R. Dennington, T. A. Keith, J. M. Millam, *GaussView, Version 6*, Semichem Inc., Shawnee Mission, KS, USA, **2016**

Entry for the Table of Contents

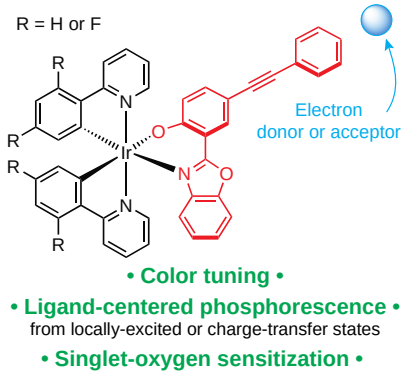

• Color tuning •
• Ligand-centered phosphorescence •
from locally-excited or charge-transfer states
• Singlet-oxygen sensitization •

The photophysical features of iridium(III) complexes incorporating an ethynyl-extended benzoxazole-based ancillary ligand are effectively modulated by the simple introduction of electron-donating (Me, NBu_2) or -withdrawing (CN) moieties on the terminal end-group, leading to CT or LC excited-states. The complexes containing the cyano-functionalized ligands features singlet oxygen sensitization parameters, making them attractive candidates for PDT.